TECHNICAL NOTE

CAUSES OF CATASTROPHIC FAILURE OF HIGH MN STEEL UTILIZED AS CRUSHER OVERLAYING SHIELDS

S. R. Allahkaram

School of Metallurgy and Materials Engineering, University Collage of Engineering
University of Tehran, P.O. Box 11155-4563, Tehran, Iran
akaram@ut.ac.ir

(Received: January 20, 2006 – Accepted in Revised Form: November 22, 2007)

Abstract The secondary cone crusher's shields at Sarcheshmeh Copper Complex of Iran are made of Hadfield steel with a nominal composition of Fe-1.3 % C-12 % Mn. They have a cut-off in the shape of a cone with an upper end diameter of 80cm and an approximate lower end diameter of 200 cm whose main problem is an unexpected early failure under normal working condition. In this paper, the results of metallographic and fractographic studies carried out on a failed shield at various depths and analytical examinations of the fractured regions are presented. It is revealed that crack propagation starts from the pre-existing microcracks in the internal regions of the shield and results in a catastrophic failure. Analytical examinations indicated other problems associated with the chemical composition of the shield. An Mn/C ratio of < 10 and high sulfur and phosphorus concentrations in the inclusions as compared to that of bulk are typical examples. The latter together with the carbide precipitation in the grain boundaries can be regarded as the pre-existing crack path in these high energy regions of the shield substructure.

Keywords Cone Crusher, Hadfield Steels, Chemical Composition, Casting, Heat Treatment, Failure, Fractography

چکیده زره‌های سنگ‌شکن‌های ثانوی در مجتمع مس سرچشمه از جنس فولاد هدفیلد با ترکیب اسمی Fe- ۱/۳ ٪ C- ۱۲ ٪ Mn می‌باشند. شکل این زره ها به صورت مخروط ناقص با قطر قسمت فوقانی ۸۰ سانتیمتر و قطر قسمت تحتانی ۲۰۰ سانتیمتر است. مهمترین مشکل این زره ها شکست غیر مترقبه و زود هنگام آنها طی شرایط عملیاتی معمول می‌باشد. در این مقاله، نتیجه مطالعات شکست نگاری و متالوگرافی بر نمونه‌های تهیه شده از زره سنگ شکن ثانوی در ضخامت‌های مختلف دیواره و از قسمت‌های ترک خورده ارائه شده است. این نتایج نشان می دهند که رشد ترک طی عملیات خردایش از طریق میکرو ترک هایی ادامه می‌یابد که بر روی سطح داخلی زره به هنگام ساخت آن بوجود می‌آید. همچنین نتایج آنالیزهای مختلف نشان می دهند که مشکل دیگر این زره‌ها در رابطه با ترکیب شیمیایی آنها بالاخص نسبت Mn/C < ۱۰ و نیز میزان بالای سولفور و فسفر در آخال ها و کاربیدها نسبت به ماتریس می‌باشد. به علاوه رسوب این آخالها در مرزدانه‌ها رشد ترک را میسر می‌سازد؛ زیرا مرز دانه‌ها نسبت به ساختار کریستالوگرافی قطعه از انرژی بالاتری برخوردار می‌باشند.

1. INTRODUCTION

High manganese steel or so called Hadfield steel is frequently used in mining. Hadfield steel has industrial applications in places where excessive deformation and wear resistance are required. Under repeated impact or abrasive wear, this alloy work-hardens rapidly and displays remarkable toughness. Due to its low yield strength, it may be deformed markedly; but it fails before the work-hardening property comes into effect [1]. This behavior can be a disadvantage in certain applications such as the case of rock-crushers [2,3].

Previous studies have attributed the strain hardening behavior of this material to its dynamic strain aging [4] or an imperfect deformation twin or so called pseudotwin [5,6]. The recent investigation proposes that interactions between dislocations and the high concentration of

interstitial atoms also contribute to additional strain hardening. Therefore, the wear resistance of Hadfield steel is related to its microstructure and hence to the heat treatment process and the subsequent water quenching effect. However, it must be noted that unless a suitable composition is obtained, the most proper heat treatment process can not produce a high quality material and the final manufactured product can not meet the expectations [7], as it has been the case of the shields under investigation.

There is only a modest amount of literatures available in failure mechanism of Hadfield steel cone crushers [8]. The majority of research studies focus on tribological behavior and wear resistance of this alloy [9,10]. Some studies have also been made of the relationship between typical microstructures and wear behavior of the materials during sliding wear [11,12]. The internal structure of these steels contains carbide and other phases which can result in lowering their toughness [13]. In the production of large parts such as cone crushers, it is not possible to prevent the formation of pearlite and carbide phases, unless the object is cooled down rapidly to the room temperature inside turbulent cold water [13].

The point which determines the final properties of the product and must be considered, particularly during fabrication process is the melted chemical composition of the cast, followed by the proper heat treatment in order to produce suitable microstructure and to prevent structural defects (voids, cracks, inclusions) and brittle phases (carbides). Therefore, various parameters such as alloying elements, casting conditions, rate of solidification, micro alloying elements and heat treatment cycles can determine optimum microstructure. It must be noted that suitable microstructure is usually formed during casting and solidification, whereas heat treatment is mainly a correction procedure. This together with the effect of overheating can prevent elemental segregation and enhanced carbide precipitation. Hence, optimization of these parameters is essential in order to produce suitable material used as cone crushers [14].

The aim of this paper is to reach an understanding on the influence of microstructure and alloying elements in catastrophic failure of the shields used as secondary cone crushers in rock mineral plant at Sarcheshmeh Copper Complex. Samples selected for this investigation were cut from a newly failed shield, which was discarded due to its fractured surface. These shields are manufactured in Iran with similar characteristics as the original shields, which were imported from abroad, years ago. At the start of this research, most shields utilized in comminuting plant, suffered similar failure after a short period of time (between 2 to 8 months). In all cases, cracks initiated from the inner surface of the lower section of the shield, where the compressive stress field (CSS) due to comminuting process was very high compared to the upper section [10]. The regions selected for metallographic studies represented typical failure characteristics among all the failed shields. The outcome of this investigation can be considered as the common cause of failure in these materials and may be applied as correction factors in fabrication of these shields.

2. BASIC PRINCIPLE OF CONE CRUSHER OPERATION

The basic principle of a cone crusher is shown in Figure 1. The main body (concave), mantle (shield) and eccentricity together, form the chamber geometry of the cone crusher.

Similar to a crank, the eccentricity turns the main shaft with constant speed. At the top, the main shaft is journaled in a pivot point. The shield is fixed to the main shaft and the concave to the crusher frame. The resulting motion of the shield

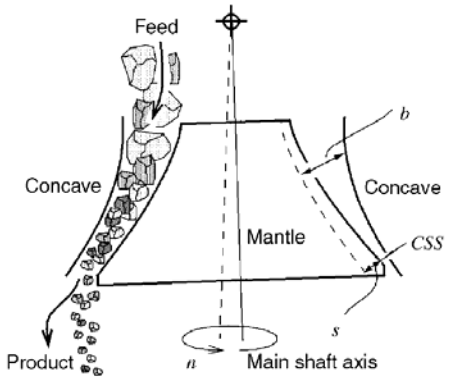

Figure 1. Schematic of cone crusher basic principle [15].

and main shaft will be a nutating motion, in which case the shield will move cyclically forward and backwards relative to the fixed main body (concave). The failure of these shields usually occurs in the lower part, where the compressive stress field (CSS) due to comminuting rock material is at its highest level.

3. EXPERIMENTAL

The chemical compositions of the core and surface of the shield obtained by quantometry analyses are given in Tables 1 and 2.

The materials used in this study were selected from the fractured regions of a newly failed shield. Also several specimens were prepared from various depths of the wall thickness of the shield for analytical examinations, using a wire cutting tool. All the specimens were prepared by standard metallographic procedures and etched with 3 % Nital reagent for about 5 seconds. For topographic and analytical examinations, a Cambridge (S360 model) scanning electron microscope (SEM) equipped with an energy dispersive x-ray spectroscopy (EDS) was used. In order to determine concentration variations of different alloying elements, line-scans were taken across the precipitated particles within the grains and grain boundaries and also at various depths below the fractured surface of the shield.

4. RESULTS AND DISCUSSION

Figures 2a and 2b show the microstructure of the internal surface layer of the shield. The micrographs taken from two different sites of the internal surface indicate inhomogeneity in the sizes of the grains at these regions. As it could be observed, some voids appeared within the grains and grain boundaries with an average diameter of 5μm scattering all over the internal surface of the shield, which were probably due to the removal of the inclusions during grinding.

Figure 3 illustrates the twin martensite branches across the boundaries of two neighboring grains of the internal subsurface layer of the shield. According to Tiantu, et al [2], although deformation twins and strain-induced martensite in the subsurface layer of a worn specimen brings about higher work-hardening capacity and hardness, which is beneficial to wear resistance, but at the same time, brittleness of work-hardened layers increases.

Figures 4a and 4b indicate the microstructures at the inner surface and at 0.5 mm below the inner surface of the shield, respectively. Figures 5a and 6a show the microstructures at 1 mm and 5 mm below the inner surface, respectively.

TABLE 1. Chemical Composition of Core of the Shield.

Element	C	Si	Mn	P	S	Cr	Ni	Mo	Cu
% Wt	1.24	0.56	13.96	0.05	0.01	1.58	0.19	1.16	0.11
Element	V	W	Ti	Co	Al	Sn	Nb	Mg	Fe
% Wt	0.09	0	0	0	0.08	0	0.14	-	Base

TABLE 2. Chemical Composition of Internal Surface of the Shield.

Element	C	Si	Mn	P	S	Cr	Ni	Mo	Cu
% Wt	1.32	0.56	12.00	0.050	0.02	1.85	0.15	1.20	0.09
Element	V	W	Ti	Co	Al	Sn	Nb	Mg	Fe
% Wt	0.02	0	0	0.01	0.046	0.01	0.10	-	82.65

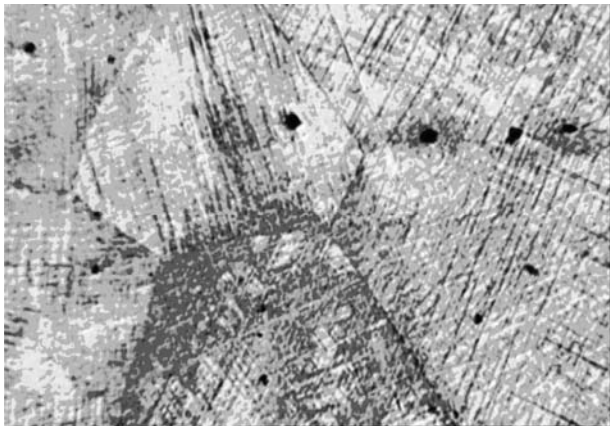

(a)

(b)

Figure 2. Two micrographs of internal surface structures of cone crusher shield at two different sites, indicating inhomogeneity in grain sizes.

Figure 3. Internal surface structure, scanning electron micrograph.

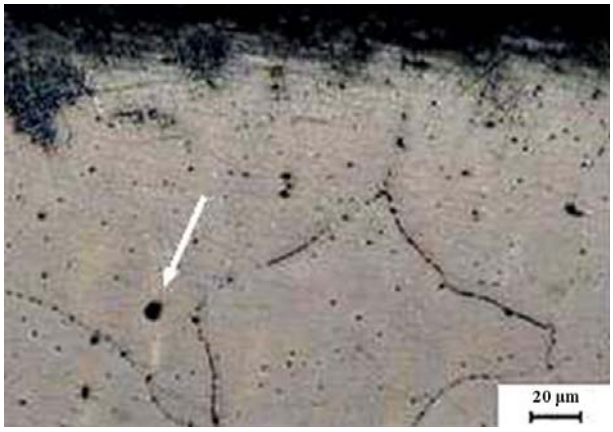

(a)

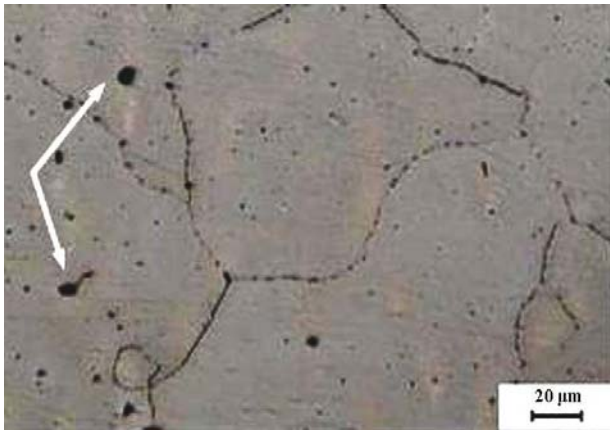

(b)

Figure 4. Structural sites near the internal surface of cone crusher shield (x-sectional traverse). (a) Close to the internal surface. (b) At 0.5 mm depth. Note the dark pits indicated by the arrows, probably due to the segregation of precipitated particles.

By comparing these figures, it can be deduced that the volume fractions of the precipitated particles increase, through the wall thickness of the shield by distancing away from the inner surface.

Although no attempt was made in order to measure the amount of volume fractions at various depths but visual examination of the cross sections at different depths, confirms this finding and by observation we see the inclusions are mostly globular in shape and are distributed all over the grains and grain boundaries. Similarly, the grains were also found to be greater in size at deeper

layers below the inner surface of the shield, compared to those at closer vicinities of the surface.

The average size of the grains at 1 mm depth was about 250 μm, which was almost twice larger than those at 0.5 mm depth (Figures 4b and 6b).

Irrespective of the cause of various grain size formations in the microstructure of the inner surface and at various depths across the wall thickness of the shield, it is a known fact that smaller grain structures can produce higher resistance to cracking, compared to the larger grains. This stems from the fact that a propagating micro crack or the movement of dislocation on slip planes can be stifled repeatedly as it encounters more barriers (grain boundaries) in the finer microstructure material [2]. Also the grain boundaries in larger microstructures usually become saturated by inclusions providing a pre-existing path for crack growth. This is due to the fact that the grain boundaries are at higher energy level, compared to the grains. Therefore, they are the preferable sites for crack propagation unless very large tensile stresses are applied in which case a cleavage fracture or transgranular failure will occur. Hence, the presence of inclusions or voids in the boundaries of larger grain microstructures can be much more serious structural defects as compared to the finer microstructures.

A more detailed examination of the crack direction revealed that the inclusions and/or the voids were preferable sites for crack propagation though the boundaries. These are illustrated in Figures 5b, 6a and 6b.

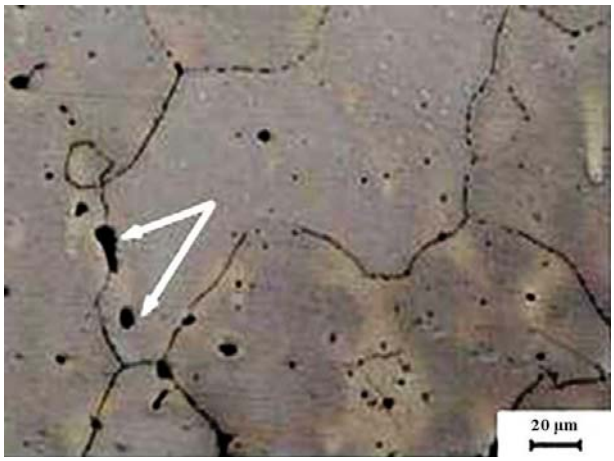

(a)

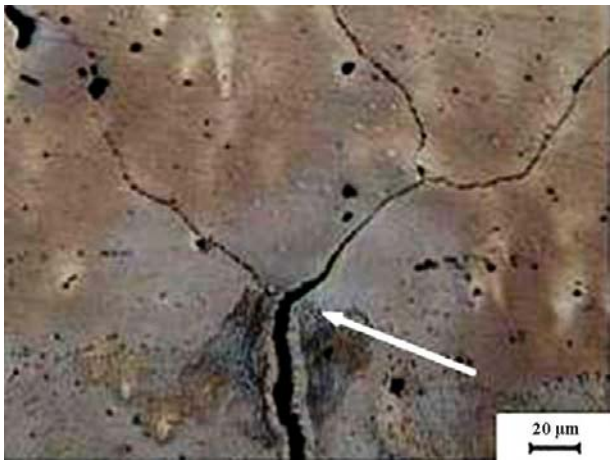

(b)

Figure 5. A grain boundary crack at (a) 1 mm depth below the internal surface and (b) 1mm depth below the surface.

5. ANALYTICAL EXAMINATION OF PARTICLE DISTRIBUTIONS WITHIN MICROSTRUCTURE

Figures 7 and 8 show the EDX spectroscopy of a precipitated particle within a grain boundary crack and in the austenitic base of the shield, respectively. By comparing these two analyses, it can be clearly observed that the presence of higher carbon content in an isolated particle within a growing crack, compared to the base metal can confirm carbide precipitation in the grain boundary. This indicates the occurrence of decarburization in close vicinity of the boundary.

For investigating elemental distributions and variations of their concentration within the material, line-scan was employed. Figures 9 and 10 illustrate the line-scan results for phosphorous taken across a grain and a grain boundary, respectively. It can be deduced from these semi-quantitative analytical results that the concentration of phosphorous within the grain boundary is almost twice as much as the concentration in the grain. Baring in mind that the phosphorous concentration in the alloy was found

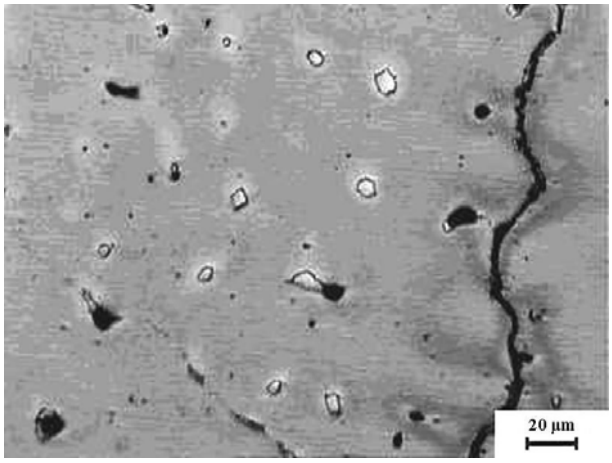

(a)

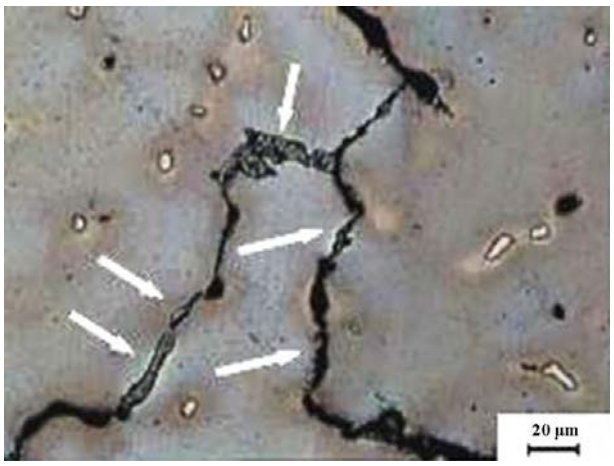

(b)

Figure 6. Microstructure at (a) 5 mm depth below the internal surface of the shield indicating internal grain boundary crack propagation and (b) precipitated particles within grain boundary crakes shown by arrows.

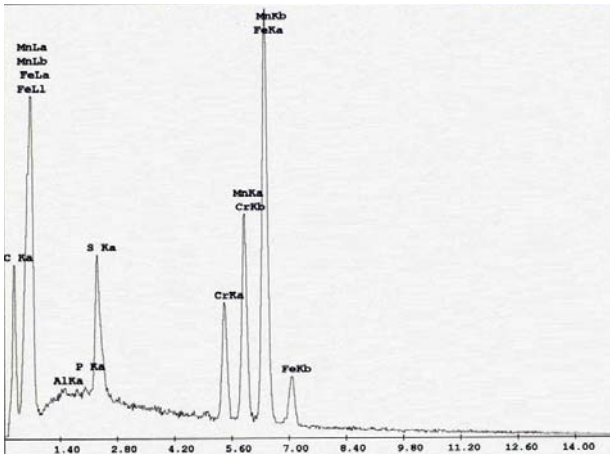

Figure 7. EDS analysis of a precipitated particle within a grain boundary crack.

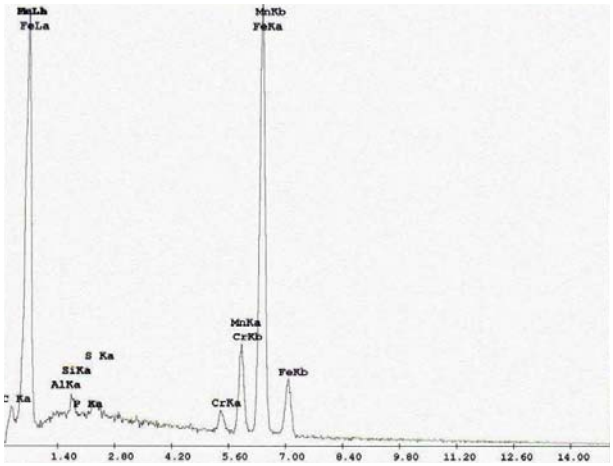

Figure 8. EDS analysis from austenitic base.

to be 0.05 % (Table 1), hence a build up of its concentration within the grain boundaries can be in excess of 0.1 %. It has been reported that phosphorous concentration over 0.05 % in Hadfield steels promote hot cracking phenomenon during fabrication process [4].

This can be further influenced due to higher concentration of interstitial sulfur diffused toward the grain boundaries. According to Figure 11, the amount of sulfur in a particle within the grain boundary is almost twice as much as the base metal.

Figures 12a, b and c illustrate the results of line-scans for variations of (a) sulfur, (b) and (c) carbon concentrations through the base metal across a crack, starting from the inner surface of the shield. The scan results indicate that phosphorous and sulfur contents within the crack are higher than those of the base metal. Figure 12c also illustrates that the variation of carbon within the crack was slightly higher than that of the base metal. These results confirm that sulfide and carbide inclusions within the grain boundaries provide available sites for a growing crack.

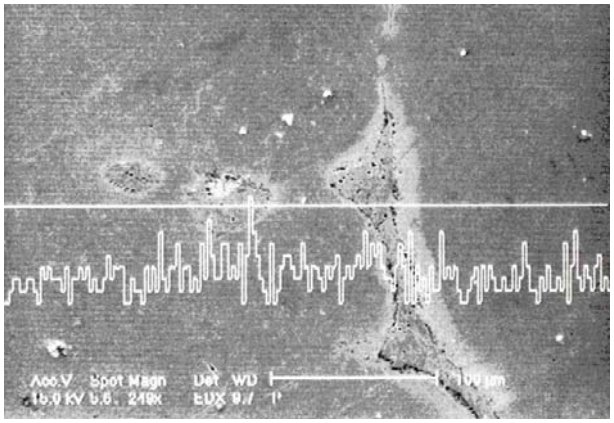

Figure 9. Phosphorous line-scan taken across a particle within a grain.

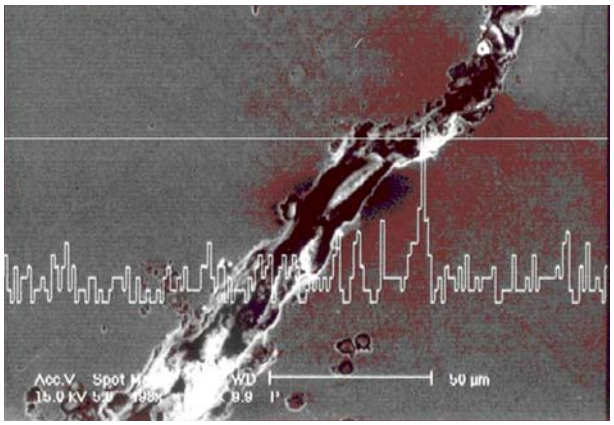

Figure 10. Phosphorous line-scan taken across a grain boundary.

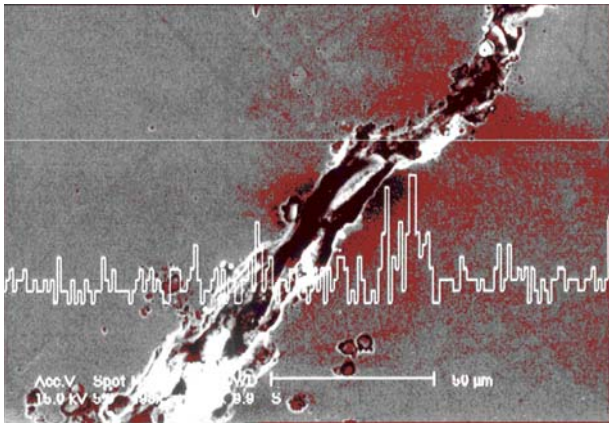

Figure 11. Sulfur line-scan taken across a particle within a grain boundary.

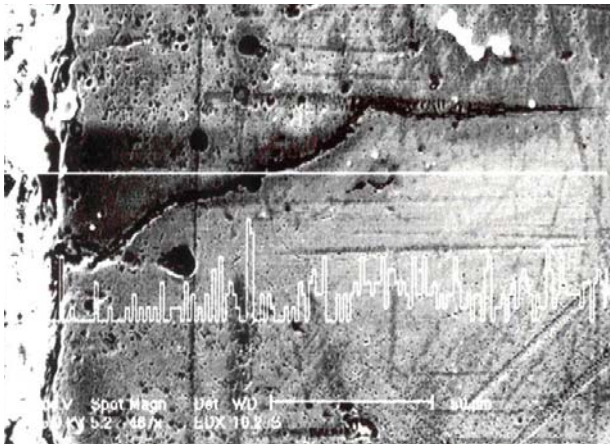

(a)

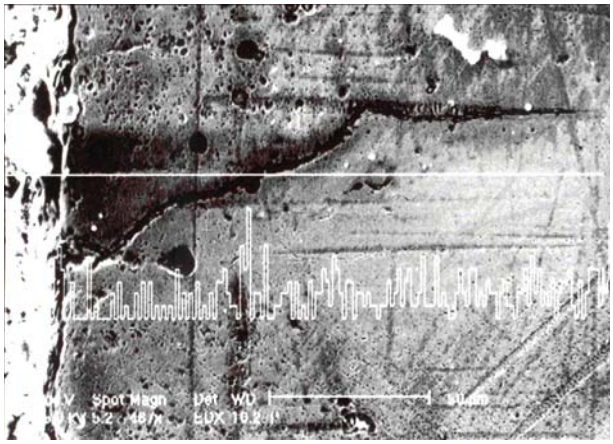

(b)

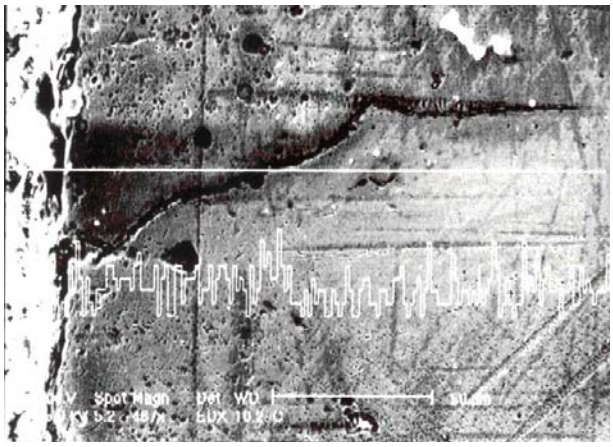

(c)

Figure 12. Variations of concentrations of (a) sulfur, (b) phosphorous and (c) carbon in a known crack path adjacent to the internal surface obtained by line-scan. Arrows show the internal surface of the shield.

Figure 13 indicates the line-scan result for carbon variations within a grain boundary at a further distance away from the internal surface of the shield. This micrograph also illustrates that the carbon content within the grain boundary is almost twice that of the base metal as well as in the vicinities adjacent to the grain boundary. Figure 14 shows the eutectoid substructure and its associated line-scan for the carbon in a selected path.

Figures 15-17 also show similar topographical analyses for sulfur, chromium and manganese concentrations, respectively. The line-scans across the eutectoid substructure for various elements indicate lower elemental contents in the eutectoid lamellar substructure than elsewhere. This finding confirms the eutectoid nature of the lamellar substructure. The depletion of alloying elements from the grains and other phases such as eutectoids and their diffusion toward the boundaries to form various inclusions within the grain boundaries result in the formation of an ideal path through which a crack can grow across the wall thickness of the shield.

For further investigation of possible decarburization and demagnetizations of the inner surface of the shield, line-scans were employed again for carbon and manganese variations from the internal surface up to 500 μm depth below the surface of the shield. Figures 18 and 19 show the results of these analyses for carbon and manganese, respectively. The distributions of these two elements can be seen to be lower near the inner surface and gradually increase through the core up to a level, after which they remain almost constant.

By comparing these figures, it can be deduced that the Mn variations from the surface through the metal is more pronounced than that of C variations along the same line.

Therefore, it is true to say that demagnetizations is a prevailing structural defect as compared to the decarburization phenomenon in these shields. This is in keeping with other investigator's findings, i.e. the ratio of Mn/C < 10 results in demagnetizations and hence failure of Hadfield steel cone crushers [8]. Hence, the propagating crack initiated from the internal surface (Figure 12), can be primarily related to the demagnetizations phenomenon.

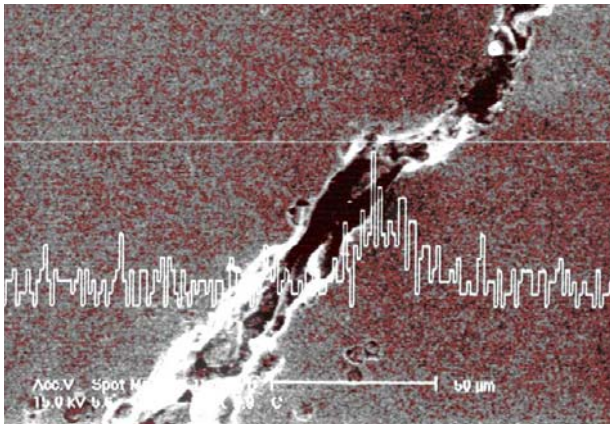

Figure 13. Carbon line-scan taken across a particle within a grain.

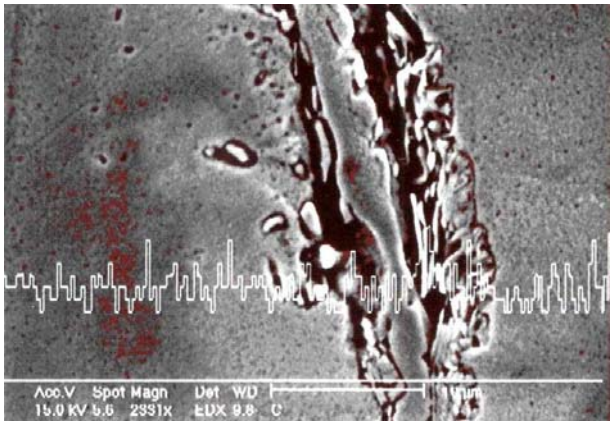

Figure 14. Carbon line-scan taken across a lamellar structure (possibly eutectoid).

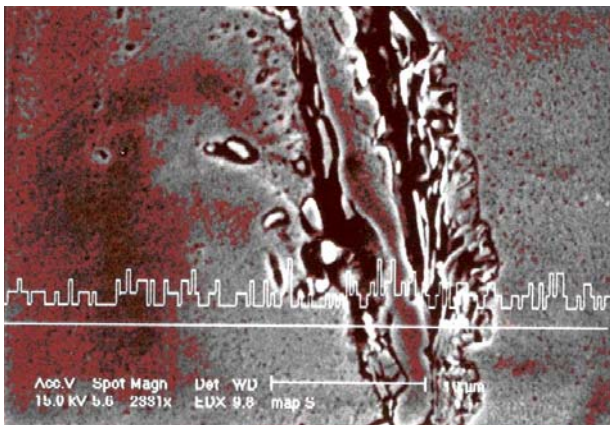

Figure 15. Concentration variations of S across eutectoid and base alloy, obtained by line-scan.

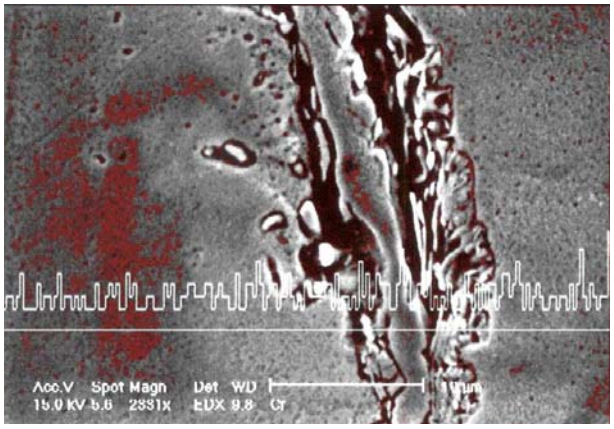

Figure 16. Concentration variations of Cr across eutectoid and base alloy, obtained by line-scan.

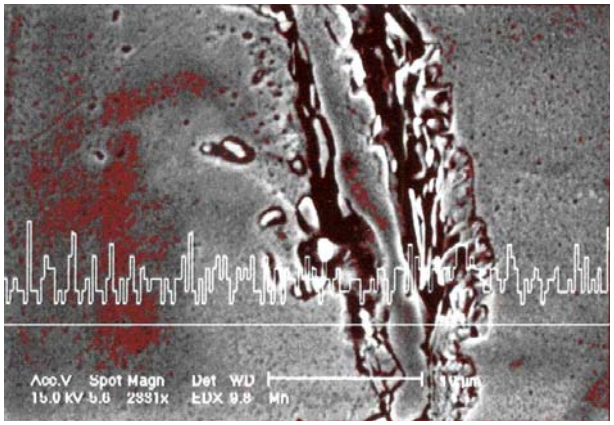

Figure 17. Concentration variations of Mn across eutectoid and base alloy, obtained by line-scan.

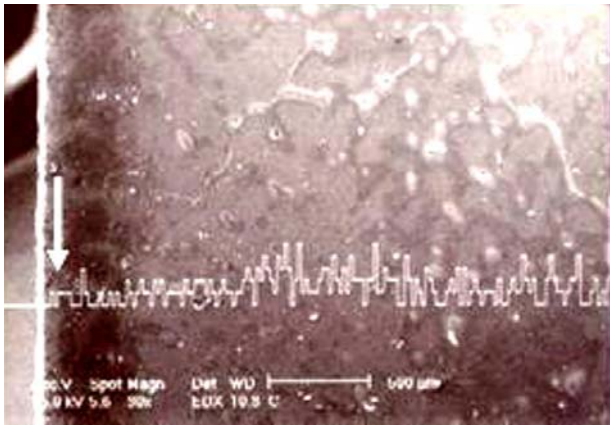

Figure 18. Concentration variations of carbon starting from the internal surface into the core, obtained by line-scan.

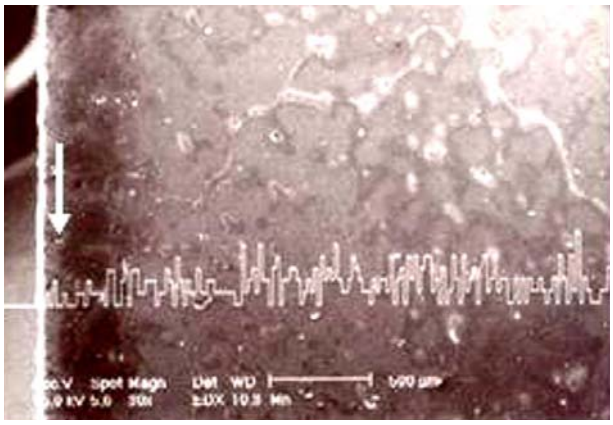

Figure 19. Concentration variations of Mn starting from the internal surface into the core, obtained by line-scan.

6. CONCLUSIONS

Samples provided from different sections along the thickness of the cone crusher shield were studied using various topographical and analytical examinations for which the following results were obtained.

Failures appeared as cracks starting from the inner surface of the shield, which was in contact with the concave main body. This was due to the demagnetizations and decarburization phenomena of the internal surface. The formation of inclusions and their subsequent precipitations within the grain boundaries provide pre-existing paths for crack initiation and its propagation along the boundaries. Analytical examinations revealed that there are high concentrations of phosphorous and sulfur in inclusions as compared to those of the matrix.

Also the ratios of $Mn/C < 10$ and $P > 0.05$ are believed to be catastrophic in chemical composition of Hadfield steels, which was the case in the shields under investigation.

Overall, it can be suggested that the early failure encountered with these shields are due to their chemical compositions and fabrication process, particularly their heat treatment and quenching conditions.

7. REFERENCES

1. Mendez, J., Ghoreshy, M. and Smith, R. W., "Weldability of Austenitic Manganese Steel", ***Journal of Materials Processing Technology***, Vol. 153, No. 154, (2004), 596-602.
2. Tianfu, J. and Fucheng, Z., "The Work-Hardening Behavior of Medium Manganese Steel under Impact Abrasive Wear Condition", ***Materials Letter***, Vol. 31, (1997), 275-279.
3. Lin, Y. C., Wang, S. W. and Chen, T. M., "A Study on the Wear Behavior of Hadfield Manganese Steel", ***Journal of Materials Processing Technology***, Vol. 120, (2002), 126-132.
4. Owen, W. S. and Grajicic, M., "Strain Aging of Austenitic Hadfield Steel", ***Acta Materialia***, Vol. 47, No. 1, (1999), 111-126.
5. Karaman, I., Sehitoglu, H., Beaudoin, A. J. and Tome, C. N., "Modeling The Deformation Behavior of Hadfield Steel Single and Polycrystals Due to Twinning and Slip", ***Acta Materialia***, Vol. 48, (2000), 2031-2047.
6. Karaman, I. Sehitoglu, H. and Kirreva, I. V., "Extrinsic Stacking Faults and Twinning in Hadfield Steel", ***Scripta Materialia***, Vol. 44, (2001), 337-343.
7. Kopac, J., "Hardening Phenomena of Mn-Austenite Steels in the Cutting Process", ***Journal of Materials Processing Technology***, Vol. 109, (2001), 96-104.
8. Jiang, Y. and Sehitolgu, H., "A Model for Rolling Contact Failure", ***Wear***, Vol. 224, (1999), 38-49.
9. Wang, Y., MC Nallan, M. and Lei, T., "Wear Resistance and Energy Consumption of Eutectoid Steel During Dry Sliding", ***Scripta Materialia***, Vol. 36, No. 2, (1997), 213-217.
10. Evertsson, C. M., "Output Prediction of Cone Crushers", ***Materials Engineering***, Vol. 11, No. 3, (1998), 215-231.
11. Kalousek, J., Fegredo, D. M. and Lauffr, E. E., "The Wear Resistance and Worn Metallography of Pearliteo Bainite and Tempered Martensite Rail Steel", ***Wear***, Vol. 105, No. 3, (1985), 199-222.
12. Wang, Y., Pan, L. and Lei, T. C., "Sliding Wear Behavior of Pearlitic Structures in Eutectoid Steel", ***Wear***, Vol. 143, No. 1, (1991), 57-69.
13. Sundstrom, A., Rendon, J. and Olsson, M., "Wear Behavior of Some Low Alloyed Steels Under Combined Impact/Abrasion Contact Conditions", ***Wear***, Vol. 250, (2001), 744-754.
14. Wang, Y., McNallan, M. and Lei, T. C., "Comparison of Dry Wear Characteristics of 2 Abrasion-Resistance Steels", ***Wear***, Vol. 36, No. 2, (1997), 213-217.
15. Lindqvist, M. and Evertsson, C. M., "Development of Wear Model for Cone Crushers", ***Wear***, Vol. 261, (2006), 435-442.